Electronic Supplementary Information

Organic emitter integrating aggregation-induced delayed fluorescence and room-temperature phosphorescence characteristics, and its application in time-resolved luminescence imaging

Fan Ni, Zece Zhu, Xiao Tong, Mingjuan Xie, Qiang Zhao,* Cheng Zhong, Yang Zou and Chuluo Yang*

Table of Contents

Experimental Procedures

1. General information

^{1}H NMR and ^{13}C NMR spectra were collected on a MECUYRVX400 spectrometer. HRMS were obtained on Thermo Scientific LTQ Orbitrap XL. UV-vis absorption spectra were recorded on a Shimadzu UV-2700 recording spectrophotometer. Fluorescence and phosphorescence emission spectra at room temperature or 77K were measured on a Hitachi F-4600 spectrophotometer. Time-gated emission spectra with delay time over 0.01 ms were measured on a PerkinElmer LS-55 spectrophotometer. Luminescent decay curves and the time-resolved emission spectra with delay time less than 0.01 ms were measured on an Edinburgh FLS920 spectrophotometer equipped with a picosecond pulsed diode laser (EPL-375, wavelength: 377nm; pulse width: 79.6 ps). Single-crystal X-ray-diffraction data for **PXZT**, **ZnPXZT1** and **ZnPXZT2** were obtained from a Bruker APEX Duo diffractometer through using MoKα radiation (λ = 0.71073 Å) or CuKα radiation (λ = 1.54178 Å). The toluene used as the solvent for the synthesis of PXZT was dried through standard procedure. The other solvents and reagents used were purchased form commercial sources and used as received without further purication. E_S and E_T were calculated from the onset of the fluorescence spectra and the phosphorescence spectra, respectively.

2. Synthesis of PXZT, ZnPXZT1 and ZnPXZT1

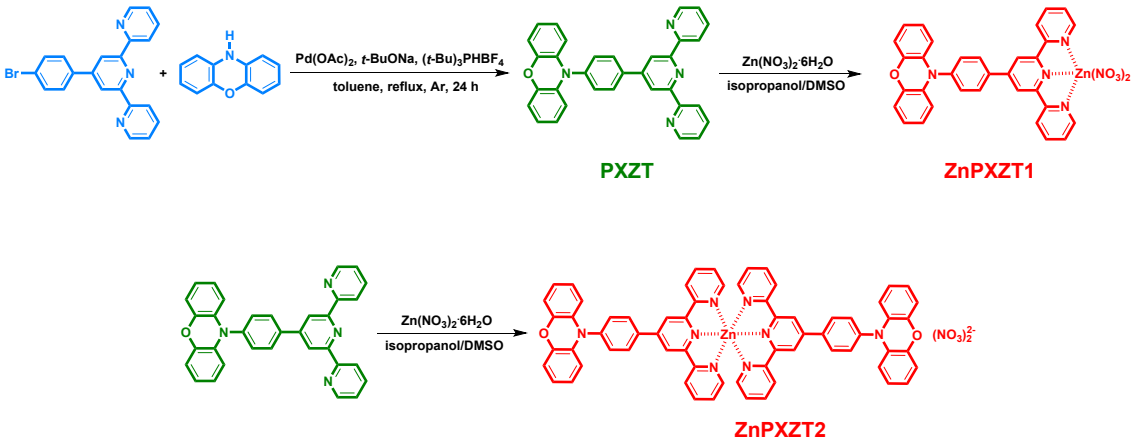

Schemes S1. The synthetic route for **PXZT**, **ZnPXZT1 and ZnPXZT2**

2.1. Synthesis of **PXZT** and the preparation of the crystal of **PXZT**

4'-(4-bromophenyl)-2,2':6',2''-terpyridine (2.33 g, 6.0 mmol), phenoxazine (1.21 g, 6.6 mmol), palladium(II) acetate (27 mg, 0.12 mmol), tri-tert-butylphosphine tetrafluoroborate (105 mg, 0.36 mmol) and sodium tert-butoxide (635 mg, 6.6 mmol) were dissolved in dry toluene (45 mL) under argon atmosphere. The mixture was stirred at reflux for 24 hours then cooled to room temperature. The mixture was then concentrated under reduced pressure. The crude product was purified by column chromatography with $CHCl_3$/methol (v/v = 100/1) as eluent, finally the brown powder PXZT was obtained with a yield of 56% (1.65 g, 3.36 mmol). The resulting product was further recrystallized from $CHCl_3$/methol to give a light yellow powder.

As for the preparation of the light yellow single crystal of PXZT, it was obtained through the slow evaporation of cyclo-hexane into a solution of PXZT in CH_2Cl_2.

^{1}H NMR (400 MHz, $CDCl_3$) δ 8.79 (s, 2H), 8.74 (d, J = 4.8 Hz, 2H), 8.70 (d, J = 8.0 Hz, 2H), 8.11 (d, J = 8.4 Hz, 2H), 7.90 (m, 2H), 7.49 (d, J = 8.4 Hz, 2H), 7.38-7.36 (m, 2H), 6.73-6.60 (m, 6H), 6.00 (m, 2H). ^{13}C NMR (100 MHz, $CDCl_3$) δ 156.14, 156.05, 149.4, 149.2, 144.0, 139.7, 138.9, 137.0, 134.2, 131.4, 130.1, 124.0, 123.4, 121.5, 121.4, 119.0, 115.5, 113.3. HRMS (ESI): m/z $[M+H]^+$ calcd for $C33H23N4O^+$: 491.1866; found: 491.1864.

2.2. Preparation of the crystal of **ZnPXZT1**

PXZT (0.102 g, 0.2 mmol) and $Zn(NO_3)_2{\cdot}6H_2O$ (0.149 g, 0.5 mmol) was dissolved in 5 mL DMSO. 20 mL isopropanol was carefully added to the above solution. After diffusion for a week, the crystals were collected, washed with isopropanol and ether, and finally dried overnight to give dark red crystals of the complex (0.129 g, yield: 95%). The crystal was directly used for single-crystal X-ray analysis.

^{1}H NMR (400 MHz, DMSO-d_6) δ 9.24 (s, 2H), 9.08 (d, J = 8.0 Hz, 2H), 8.92 (d, J = 4.8 Hz, 2H), 8.56 (d, J = 8.4 Hz, 2H), 8.46 (t, J = 8.4 Hz, 2H), 8.01-7.96 (m, 2H), 7.78 (d, J = 8.4 Hz, 2H), 6.84-6.79 (m, 6H), 6.00-5.98 (m, 2H). ^{13}C NMR (75 MHz, DMSO-d_6) δ153.9, 149.4, 148.4, 147.8, 143.7, 141.8, 141.2, 134.0, 132.0, 131.7, 128.2, 124.3, 124.1, 122.3, 121.2, 116.0. HRMS (ESI): m/z (M-$^{2NO_3^-}$)$^{2+}$ calcd for $C_{33}H_{22}N_4OZn^{2+}$: 277.0537; found: 277.0532.

2.3. Preparation of the crystal of **ZnPXZT2**

PXZT (147 mg, 0.30 mmol) and $Zn(NO_3)_2{\cdot}6H_2O$ (45 mg, 0.15 mmol) was dissolved in 8 mL DMSO. 20 mL isopropanol was carefully added to the above solution. After diffusion for a week, the red crystals (147 mg, yield: 84%) were collected and used for single-crystal X-ray analysis.

^{1}H NMR (400 MHz, DMSO-d_6), δ (ppm) 9.51 (s, 4H), 9.19 (d, J = 8.0 Hz, 4H), 8.71 (d, J = 8.4 Hz, 4H), 8.33 (t, J = 8.0 Hz, 4H), 7.98 (d, J = 4.4 Hz, 4H), 7.89 (d, J = 8.4 Hz, 4H), 7.54 (t, J = 6.4 Hz, 4H), 6.85-6.75 (m, 12H), 6.02 (t, J = 4.8 Hz, 4H). ^{13}C NMR (100 MHz, DMSO-d_6) δ 154.7, 150.0, 148.3, 148.2, 143.7, 141.9, 141.4, 136.4, 134.1, 132.1, 131.8, 128.3, 124.3, 124.1, 122.4, 122.0, 116.1, 113.7. HRMS (ESI): m/z (M-$^{2NO_3^-}$)$^{2+}$calcd for $C_{66}H_{44}N_8O_2Zn$: 522.1434; found: 522.1437.

3. Cell cytotoxicity

The cytotoxicity was measured using a standard methyl thiazolyl tetrazolium (MTT, Sigma Aldrich) assay in HeLa cell lines. Briefly, cells growing in log phase were seeded into 96-well cell culture plate at 1×10^4/well. ZnPXZT1 was added to the wells of the treatment group at concentrations of 10, 20, 30, 40 and 50 μM. The cells were incubated for 24 h at 37°C under 5% CO_2. The combined MTT/PBS solution was added to each well of the 96-well assay plate and incubated for an additional 4 h. After removal of the culture solution, 200 μL DMSO was added to each well, shaking for 10 min at shaking table. An enzyme-linked immunosorbent assay (ELISA) reader was used to measure the OD570 (absorbance value) of each well referenced at 490 nm. The following formula was used to calculate the viability of cell growth:

Viability (%) = (mean of absorbance value of treatment group / mean of absorbance value of control) × 100.

4. Cell imaging

Confocal luminescence imaging was carried out on an Olympus IX81 laser scanning confocal microscope equipped with a 40 immersion objective len. A semiconductor laser at 405 nm was served as excitation. The HeLa or 3T3 cells were incubated with the ZnPXZT1 (10 μM) for 5 h at 37 °C. Then the cells were washed with PBS (phosphate buffer saline) for three times and transferred into Live Cell Imaging System (OLYMPUS, Xcellence) for confocal luminescence imaging.

The time-gated luminescence imaging setup is integrated with Olympus IX81 laser scanning confocal microscope. The luminescence signals were detected by confocal microscope system and the correlative calculation of the data was performed using professional software which was provided by PicoQuant GmbH. The excitation light of 405 nm with a frequency of 0.5 MHz from the pulse diode laser (PicoQuant, PDL 800-D) was focused onto the sample with a 40 X objective lens (NA 0.95) for single-photon excitation.

Results and Discussion

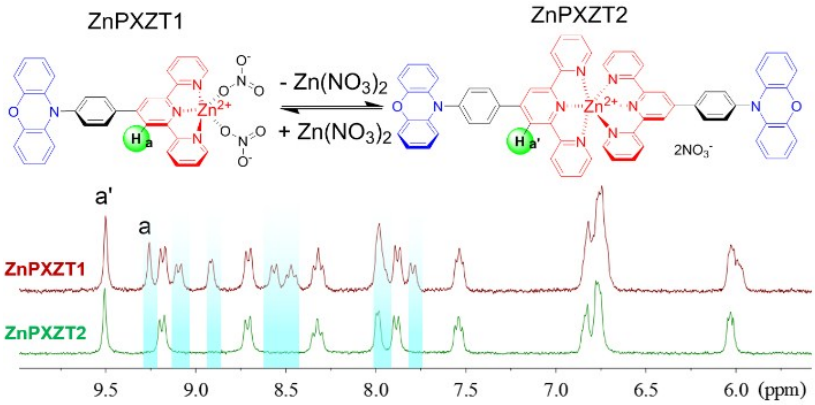

Figure S1. The ^{1}H NMR spectrum of the complex **ZnPXZT1** in DMSO-d_6. The result showed more peaks than expected that a chemical equilibrium between **ZnPXZT1** and **ZnPXZT2** was considered to be the reason. Due to the ^{1}H-NMR spectra in DMSO-d_6, [**ZnPXZT1]:** [**ZnPXZT2]** ≈ 2:3.

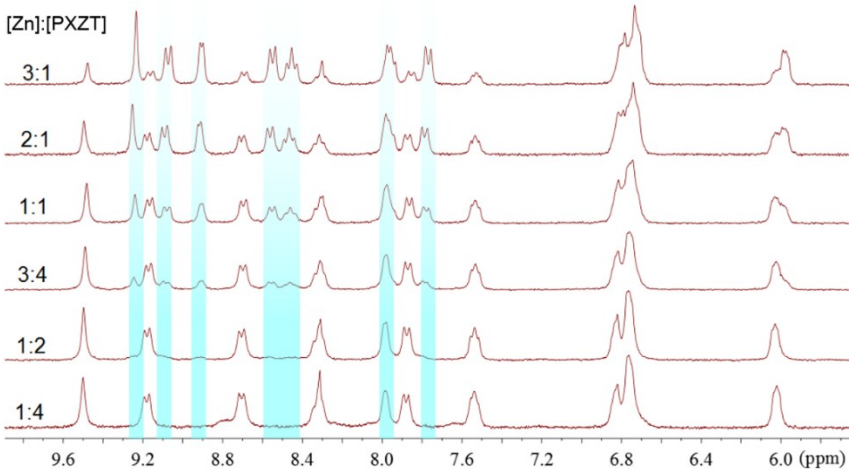

Figure S2. The ^{1}H-NMR spectra of **PXZT** in the presence of different equivalence ratios of znic nitrate in DMSO. When the equivalence ratio of ligand to zinc ion was 2:1, there were about ten sets of NMR peaks, which can be assigned to eleven kinds of H atoms of the **PXZT**. As the ratio of zinc ion increased, six sets of new NMR peaks appeared, which were assigned to the H of the 1:1 complex. Even when the concentration of zinc nitrate was three fold of the ligand, the 2:1 complex still existed in this solution. The titration results well provided the evidence of the chemical equilibrium between **ZnPXZT1** and **ZnPXZT2** in DMSO-d_6.

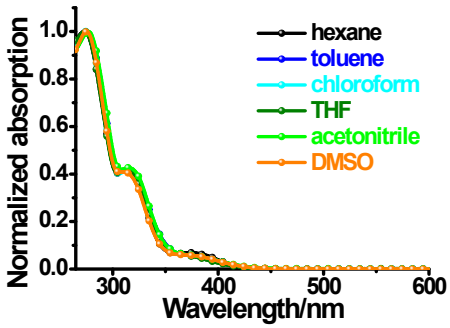

Figure S3. Normalized absorption spectra of **PXZT** in different solutions at room temperature. λ_{ex} = 370 nm.

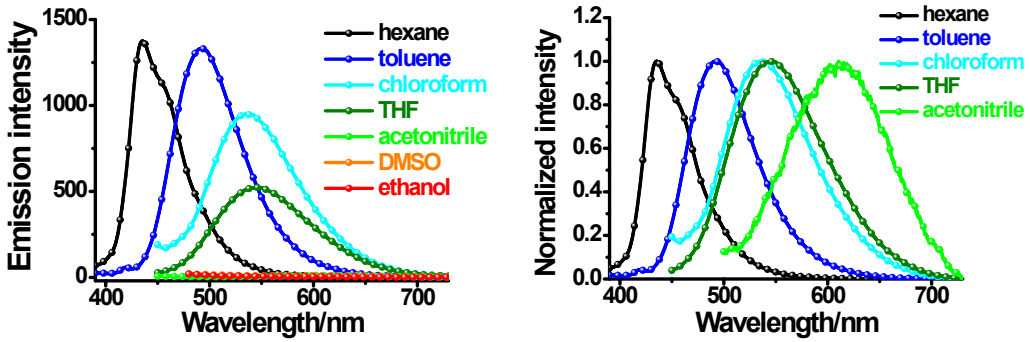

Figure S4. Steady-state emission spectra of 20 μM **PXZT** in different solutions at room temperature. λ_{ex} = 370 nm.

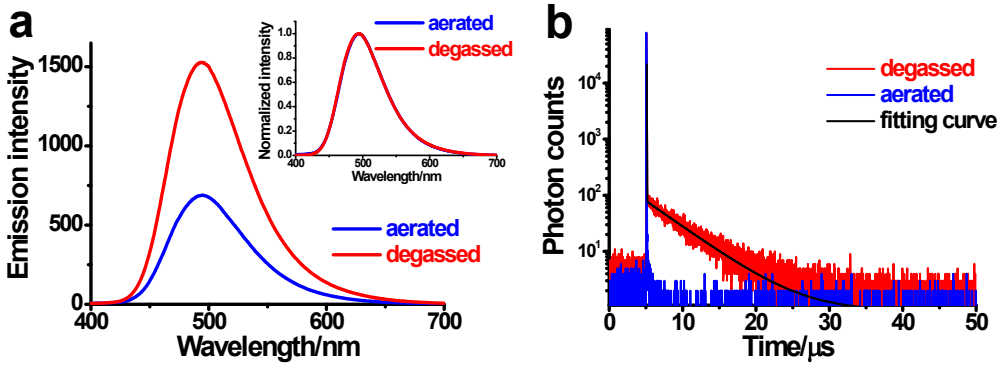

Figure S5. Steady-state emission spectra (a) and transient photoluminescence decay spectra (b) of **PXZT** in toluene solution at room temperature with and without degassing with argon. λ_{ex} = 377 nm. λ_{em} = 500 nm.

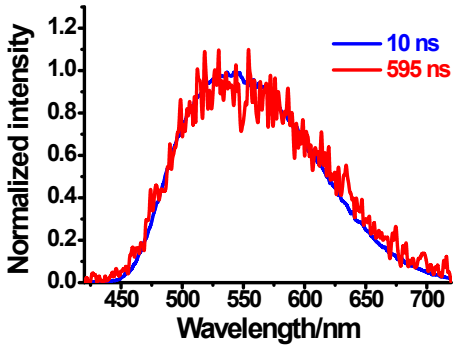

Figure S6. Time-resolved emission spectra of **PXZT** in 2-methyltetrahydrofuran solution at room temperature after degassing with argon. λ_{ex} = 377 nm, λ_{em} = 377 nm.

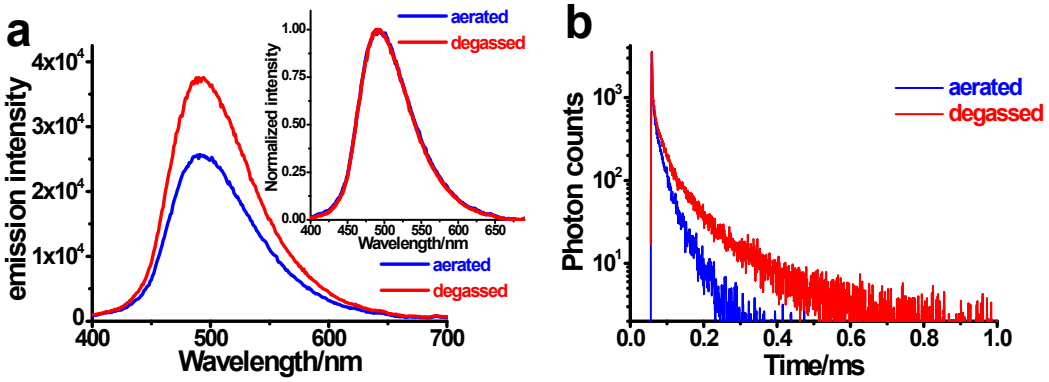

Figure S7. Steady-state emission spectra (a) and transient photoluminescence decay spectra (b) of **PXZT** in PMMA film at room temperature without and after degassing with argon. λ_{ex} = 370 nm. λ_{em} = 491 nm.

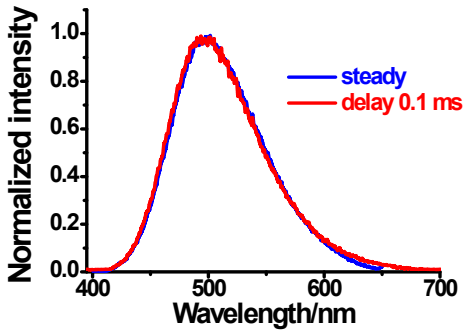

Figure S8. Steady-state and time-gated emission spectra of **PXZT** in PMMA film at room temperature under air, λ_{ex} = 370 nm.

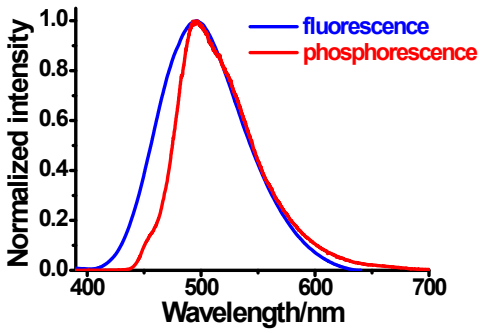

Figure S9. The emission spectra of **PXZT** in PMMA film at 77K. λ_{ex} = 370 nm. E_S = 2.88 eV, E_T = 2.70 eV, ΔE_{ST} = 0.18 eV. E_S and E_T were calculated from the onset of the fluorescence spectra and the phosphorescence spectra, respectively.

Table S1. The lifetimes and the ratio of prompt and delay fluorescence of **PXZT** in THF/H_2O.

f_w[a][b]	τ_p/Ratio [ns]/[%][c]	τ_d/Ratio [ns]/[%][d]
0	10.6/100	-/-
10	9.1/100	-/-
20	6.2/100	-/-
30	2.9/100	-/-
40	10.5/100	-/-
50	10.8/100	-/-
60	11.7/95	156/5
70	10.3/91	200/9
80	21.0/87	1352/13
90	19.9/83	1394/17

[a] Water fractions. [b] Measured under air condition at 506 nm. [c] The lifetimes and the ratios of the prompt fluorescence. [d] The lifetimes and ratios of the delayed fluorescence.

Table S2. The lifetimes and the ratio of prompt and delay fluorescence of different concentration of **PXZT** in THF/H_2O (v/v = 1/9).

Concentration of **PXZT** (μM)	τ_p/Ratio [ns]/[%][a][b]	τ_d/Ratio [ns]/[%][a][c]
1	17.1/91	331/9
2	26.4/91	478/9
5	21.3/88	849/12
10	21.8/85	1375/15
20	19.9/83	1394/17

[a] Measured under air condition at 506 nm. [b] The lifetimes and the ratios of the prompt fluorescence. [c] The lifetimes and ratios of the delayed fluorescence.

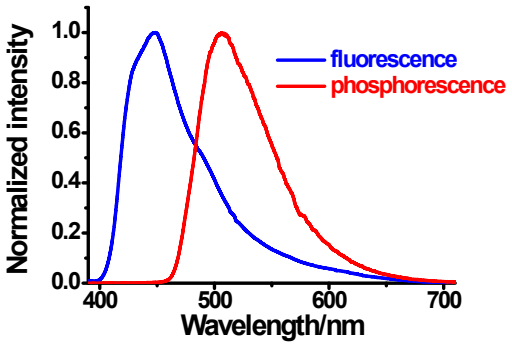

Figure S10. The emission spectra of the crystal of **PXZT** at 77K. λ_{ex} = 370 nm.

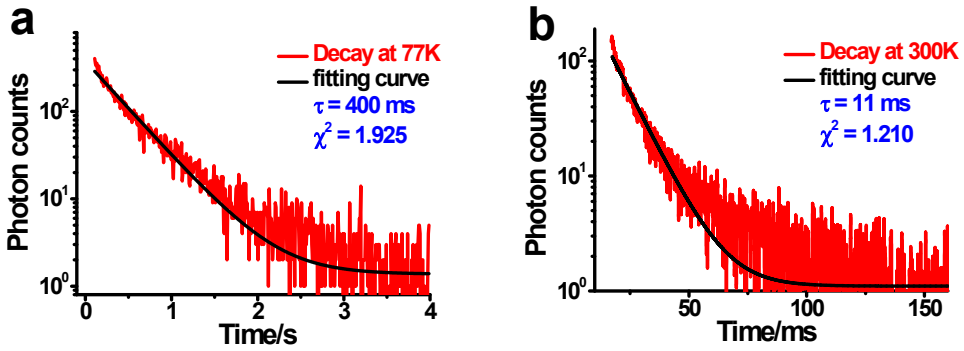

Figure S11. Transient photoluminescence decay spectra of the crystal of **PXZT** at 77K (a) and 300K (b). λ_{ex} = 370 nm. λ_{em} = 560 nm.

Table S3. The summarized photophysical data of PXZT in 2-methyltetrahydrofuran, aggregates in THF/H_2O (f_w = 90%), PMMA film and crystal state.

State	Wavelength [nm]	τ_p/τ_d [ns]/[μs][e]
In 2-methyltetrahydrofuran[a]	540[c]	17/0.9
In THF/H_2O (f_w = 90%)[b]	506[c]	20/1.4
In PMMA film[a]	491[c]	-/176
In crystal state[b]	496[c]/560[d]	-/11000

[a] Measured under argon condition. [b] Measured under air condition. [c] The measured fluorescence peak. [d] The measured phosphorescence peak. [e] The measured lifetimes.

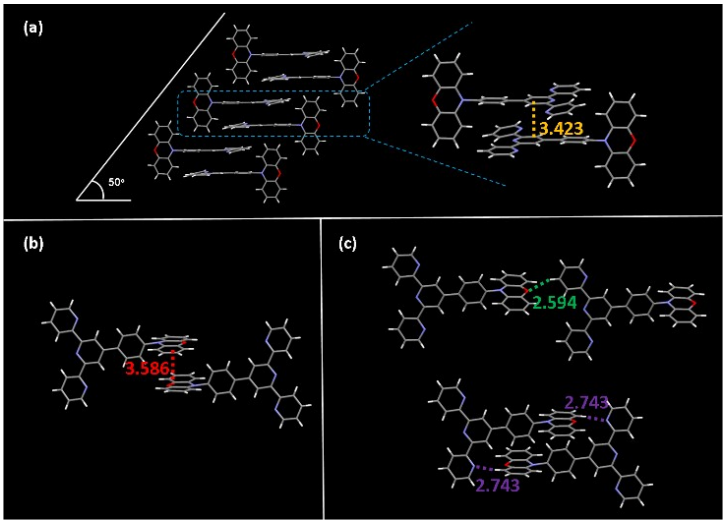

Figure S12. (a)-(c) View of the stacking and hydrogen bonding extracted from the crystal structure. Colour code: carbon = grey, hydrogen = white, nitrogen = blue, oxygen = red. Terpyridyl-terpyridyl stacking (orange dashed line), **PXZ-PXZ** stacking (red dashed line), C-H···O hydrogen bond (green dashed line) and C-H···N hydrogen bonds (purple dashed lines).

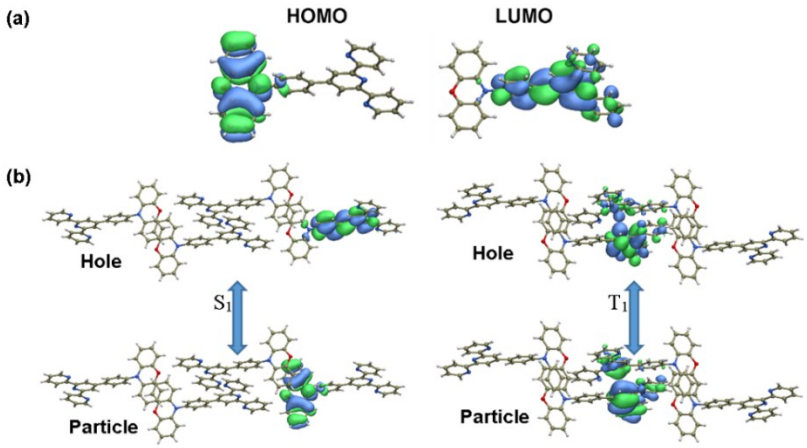

Figure S13. (a) The calculated HOMO and LUMO of one **PXZT** molecule that extracted from the crystal structure. The ground state optimization was investigated by density functional theory (DFT) calculations at the B3LYP/6-31G(d) level. (b) The NTO distributions of S_1 and T_1 state of the aggregate with four **PXZT** molecules extracted from the crystal structure were applied in CAM-B3LYP/6-31G(d) level.

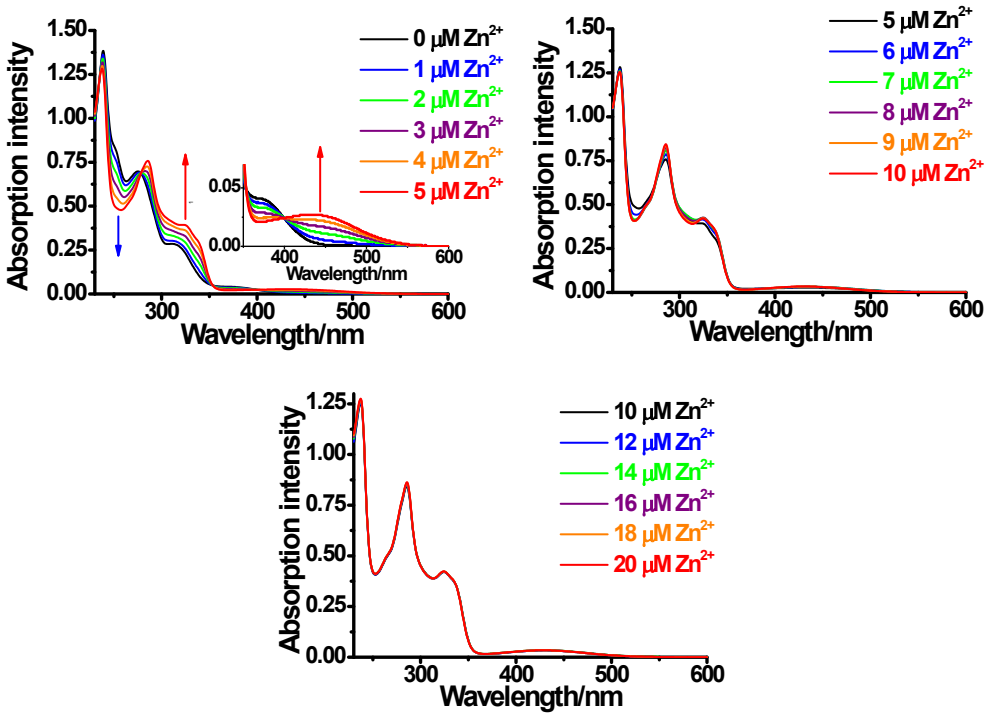

Figure S14. Absorption spectra of 10 μM **PXZT** upon addition of $Zn(NO_3)_2{\cdot}6H_2O$ in ethanol at room temperature under air.

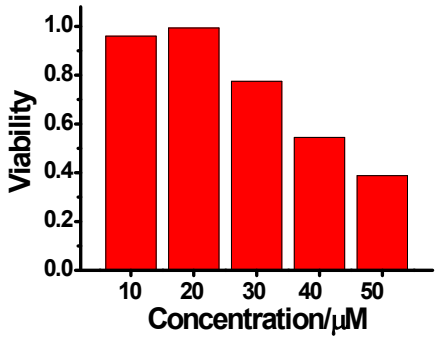

Figure S15. Cell viability values (%) assessed using an MTT (methyl thiazolyl tetrazolium) proliferation test versus incubation concentrations of **ZnPXZT1**. HeLa cells were cultured in the presence of 0-50 μM **ZnPXZT1** at 37°C for 24 h. After incubation with **ZnPXZT1** for 24 h, the cell viability was above 90% when the concentration of the complex was below 20 μM. This indicated a good biocompatibility of **ZnPXZT1** at low concentration.

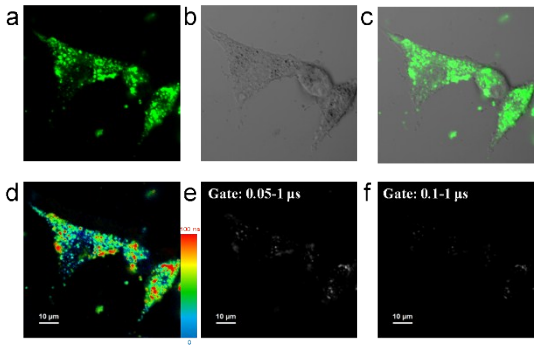

Fig. S16 Steady-state (a-c), luminescence lifetime (d) and time-gated (e, f) imaging of 3T3 cells incubated with 10 μM ZnPXZT1. λ_{ex} = 405 nm, λ_{em} = 470-570 nm. (a) Darkfield; (b) bright field; (c) merging of (a) and (b).

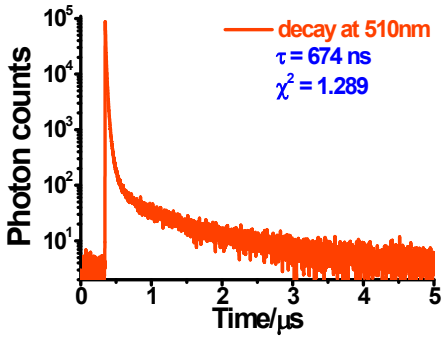

Figure S17. Transient photoluminescence decay spectra of 20 μM of **ZnPXZT1** upon addition of 50 μM EDTA in 10 mM HEPES (pH = 7) buffer in air. λ_{ex} = 377 nm. λ_{em} = 510 nm.

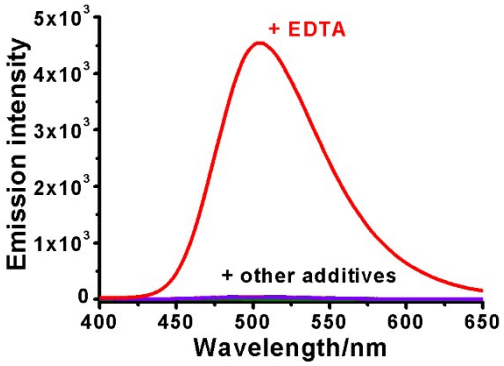

Figure S18. Steady-state emission spectra of 20 μM of **ZnPXZT1** solution upon addition of 50 μM additives in HEPES buffer at room temperature under air. λ_{ex} = 330 nm. Other additives = Cl^-, Br^-, I^-, OH^-, SH^-, OAc^-, NO_2^-, NO_3^-, SO_3^{2-}, SO_4^{2-}, CO_3^{2-}, PO_4^{3-}, HPO_4^{2-}, $Cr_2O_7^{2-}$, ppi, Cys, Gly, Ala, Val, Leu, Ile, Pro, Phe, Tyr, Trp, Ser, Thr, Met, Asn, Asp, Gln, Glu, Lys, Arg, His, Cit.

Table S4. The comparison between **ZnPXZT1**with the existing bench marks for TADF-based TRLI.

Compound	Small molecule or nanoparticle	Structural complexity	Self-luminescence or not	Turn-on detection	aggregation-induced emission enhancement	aggregation-induced TADF enhancement	Additional assistance or preparation	reference
DCFMPYM	small molecule	complicated	Yes	No	No	No	Yes	1
DCFMPYM-thiol	small molecule	complicated	Yes	Yes	No	No	Yes	2
CPy	nanoparticle	simple	Yes	No	Yes	No	Yes	3
3	small molecule	complicated	Yes	No	No	No	Yes	4
BP-PTZ BP-2PTZ	nanoparticle	simple	Yes	No	Yes	No	Yes	5
ZnPXZT1	small molecule	simple	No	Yes	Yes	Yes	No	Present work

References

1. X. Xiong, F. Song, J. Wang, Y. Zhang, Y. Xue, L. Sun, N. Jiang, P. Gao, L. Tian and X. J. Peng, *J. Am. Chem. Soc*. 2014, **136**, 9590-9597.
2. X. Xiong, L. Zheng, J. Yan, F. Ye, Y. Qian and F. Song, *RSC Adv.*, 2015, **5**, 53660-53664.
3. T. Li, D. Yang, L. Zhai, S. Wang, B. Zhao, N. Fu, L. Wang, Y. Tao and W. Huang, *Adv. Sci*. 2017, **4**, 1600166.
4. Y. Wu, F. Song, W. Luo, Z. Liu, B. Song and X. Peng, *ChemPhotoChem* 2017, **1**, 79-83.

5. S. Gan, J. Zhou, T. A. Smith, H. Su,W. Luo, Y. Hong, Z. Zhao and B. Z. Tang, *Mater. Chem. Front.*, 2017, **1**, 2554-2558.

^{1}H and ^{13}C NMR spectra of PXZT, ZnPXZT1 and ZnPXZT2

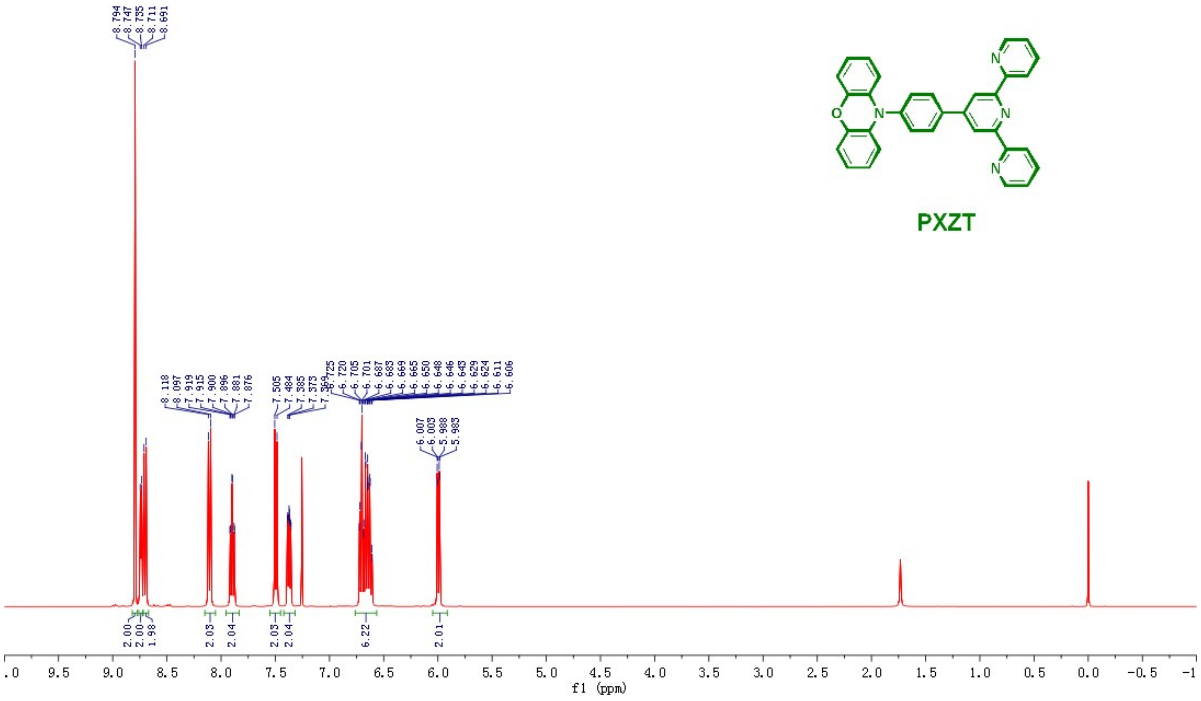

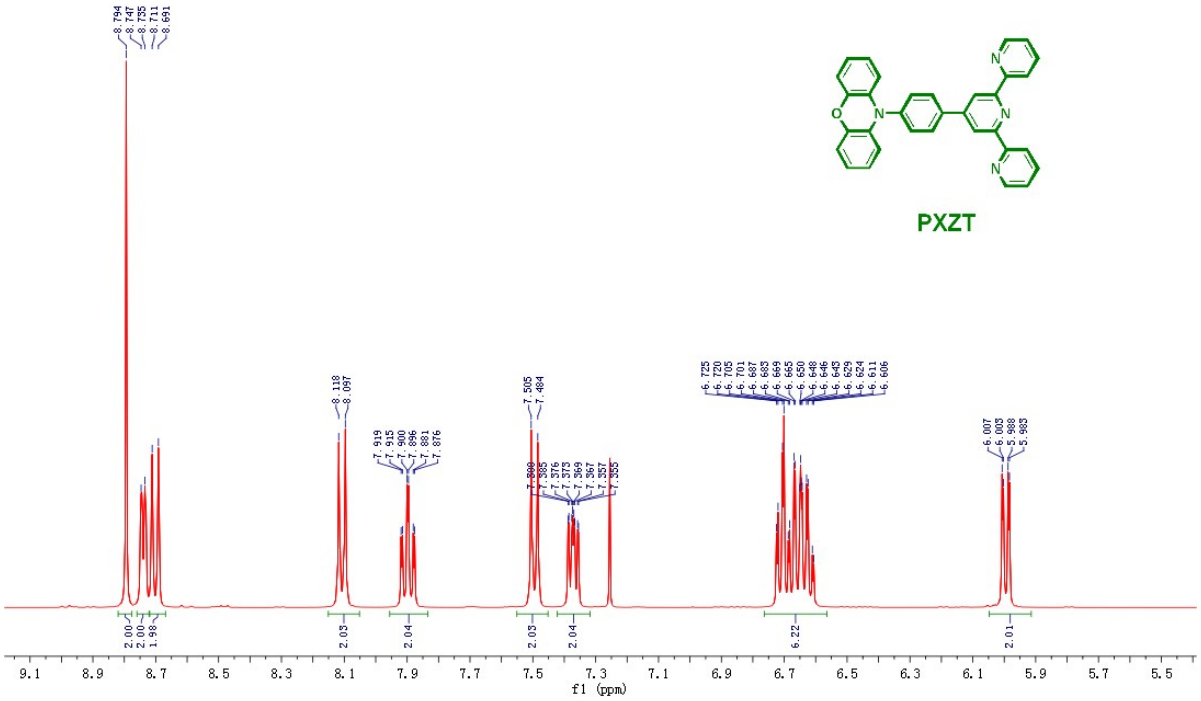

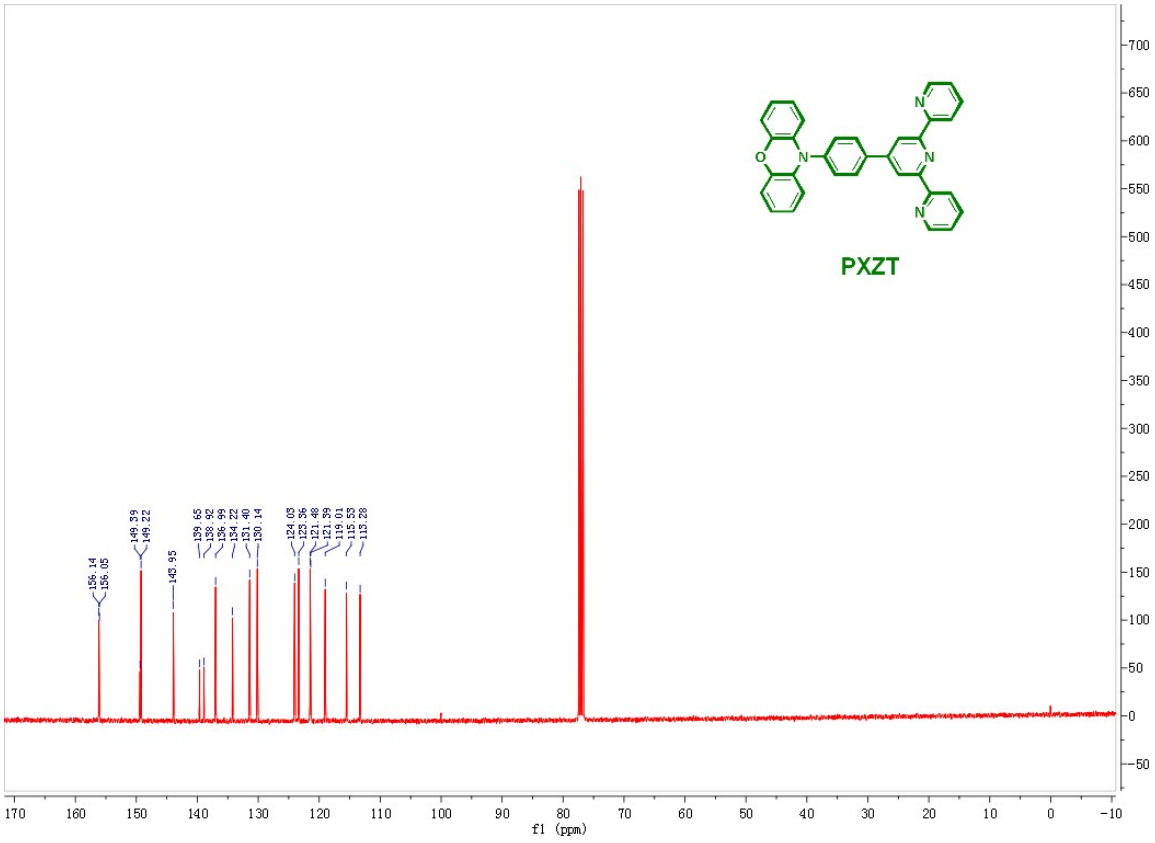
PXZT
156.14
156.05
149.39
149.22
145.95
139.65
138.92
136.99
134.22
131.40
130.14
124.03
123.36
121.48
121.39
119.01
115.53
113.28
f1 (ppm)

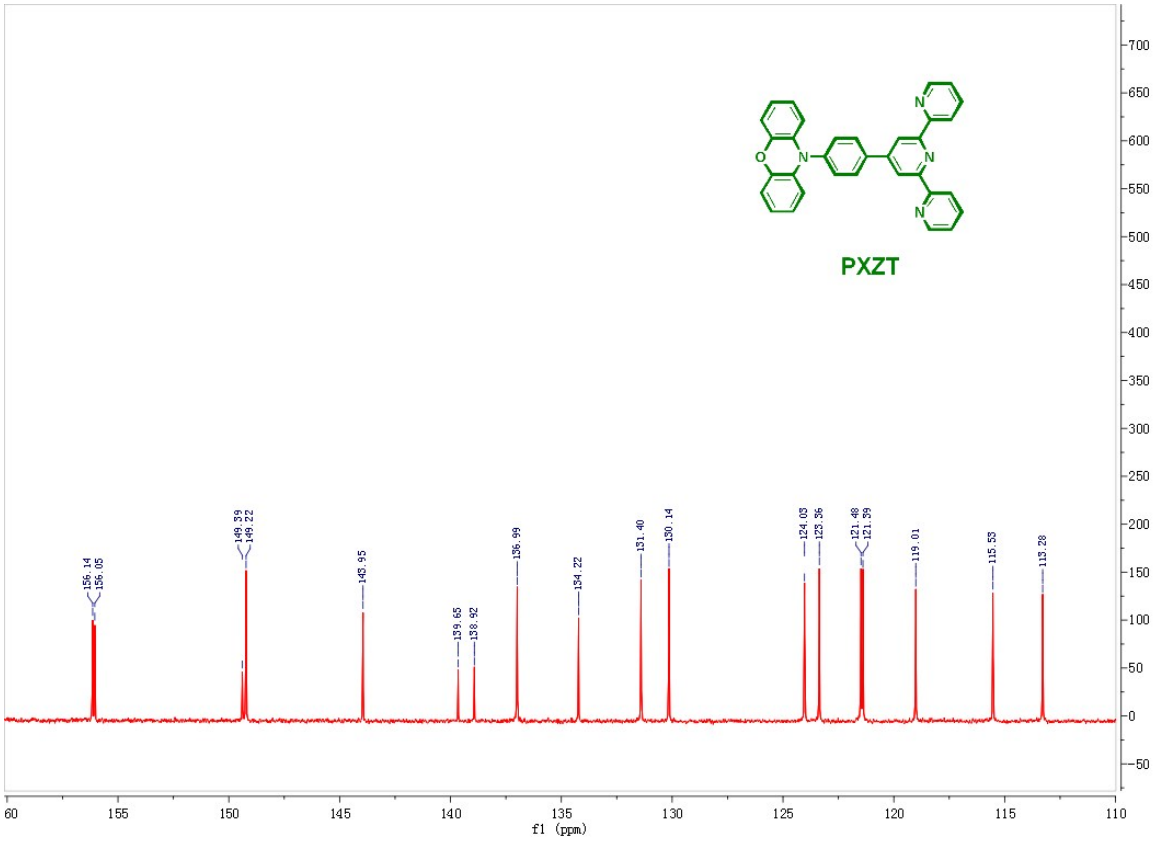
PXZT
156.14
156.05
149.39
149.22
145.95
139.65
138.92
136.99
134.22
131.40
130.14
124.03
123.36
121.48
121.39
119.01
115.53
113.28
f1 (ppm)

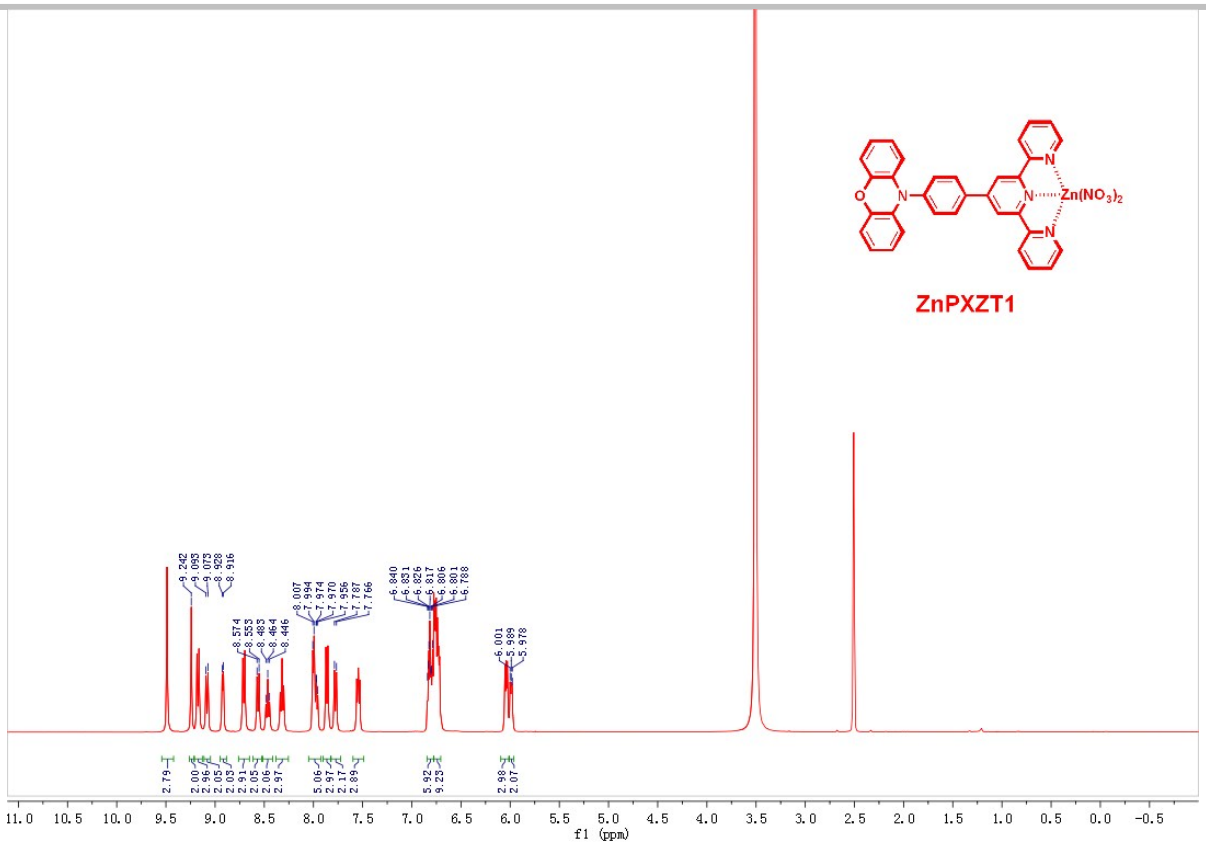
ZnPXZT1
f1 (ppm)

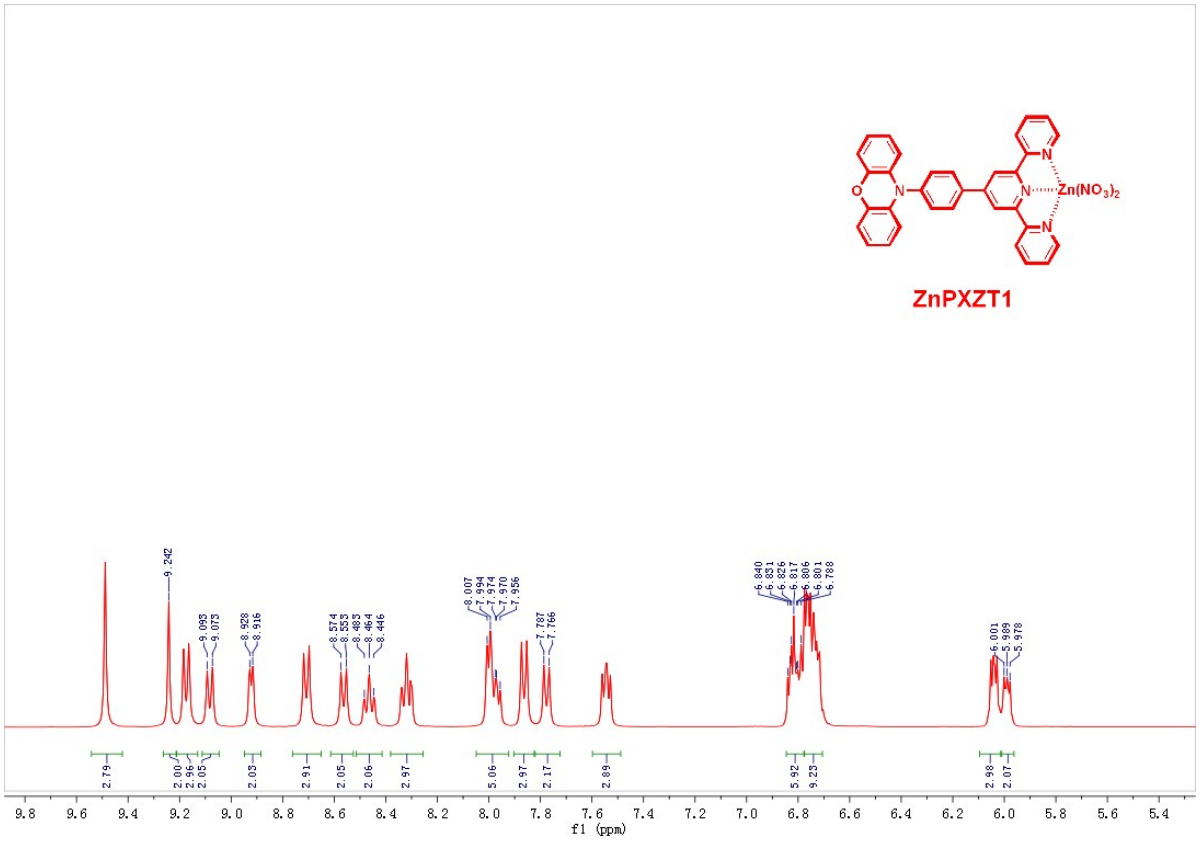
ZnPXZT1
f1 (ppm)

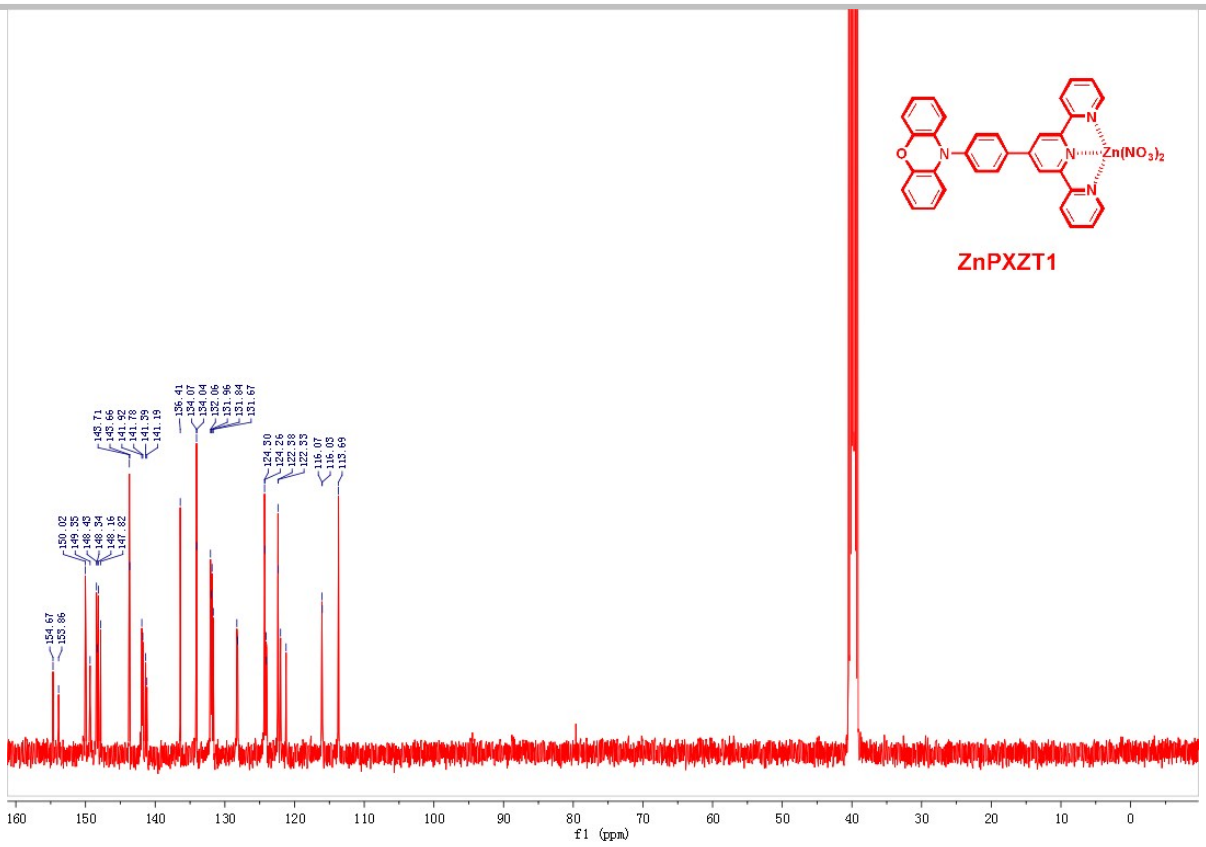
ZnPXZT1
154.67
153.86
150.02
149.35
148.43
148.34
148.16
147.82
143.71
143.66
141.92
141.78
141.59
141.19
136.41
134.07
134.04
132.06
131.96
131.84
131.67
124.30
124.26
122.38
122.33
116.07
116.03
113.69
f1 (ppm)

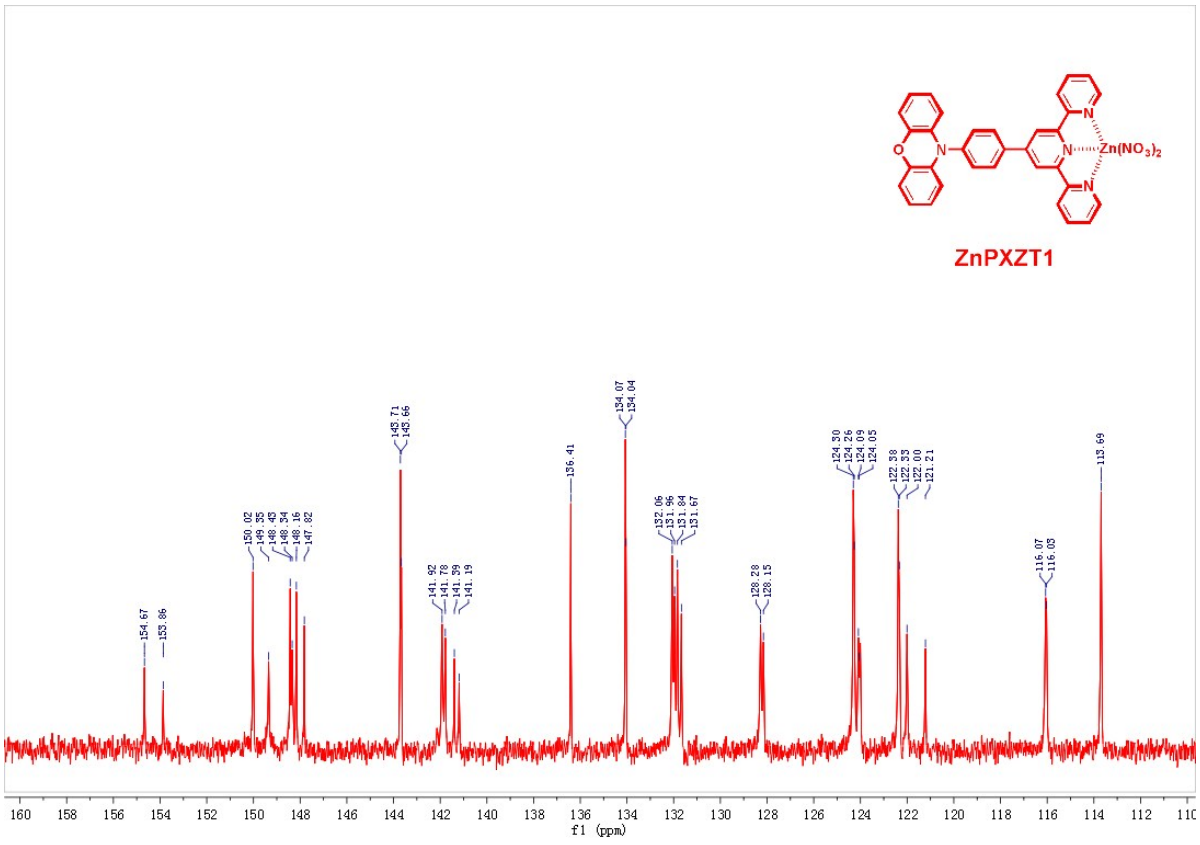
ZnPXZT1
154.67
153.86
150.02
149.35
148.43
148.34
148.16
147.82
143.71
143.66
141.92
141.78
141.59
141.19
136.41
134.07
134.04
132.06
131.96
131.84
131.67
128.28
128.15
124.30
124.26
124.09
124.05
122.38
122.33
122.00
121.21
116.07
116.05
113.69
f1 (ppm)

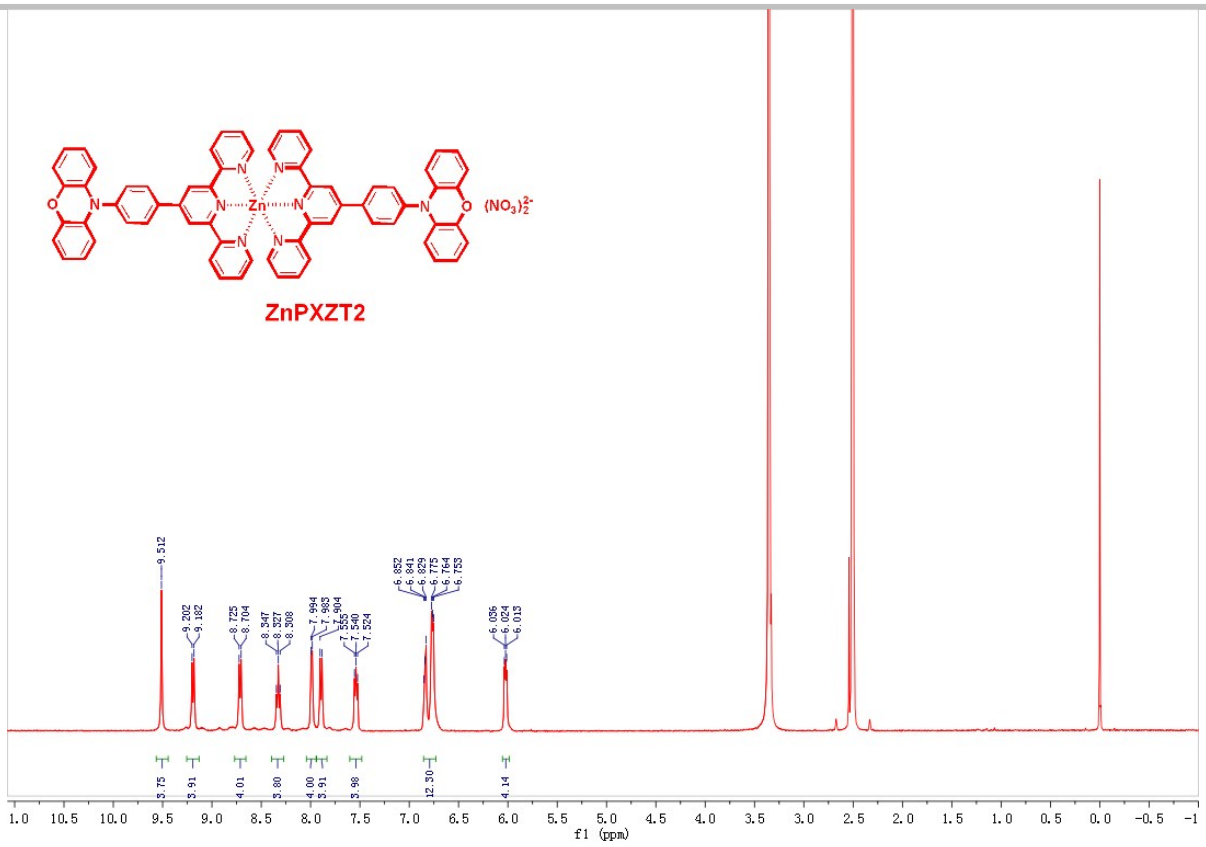
ZnPXZT2
(NO3)2
9.512
9.202
9.182
8.725
8.704
8.347
8.327
8.308
7.994
7.983
7.904
7.555
7.540
7.524
6.852
6.841
6.829
6.775
6.764
6.753
6.036
6.024
6.013
3.75
3.91
4.01
3.80
4.00
3.91
3.98
12.30
4.14
f1 (ppm)

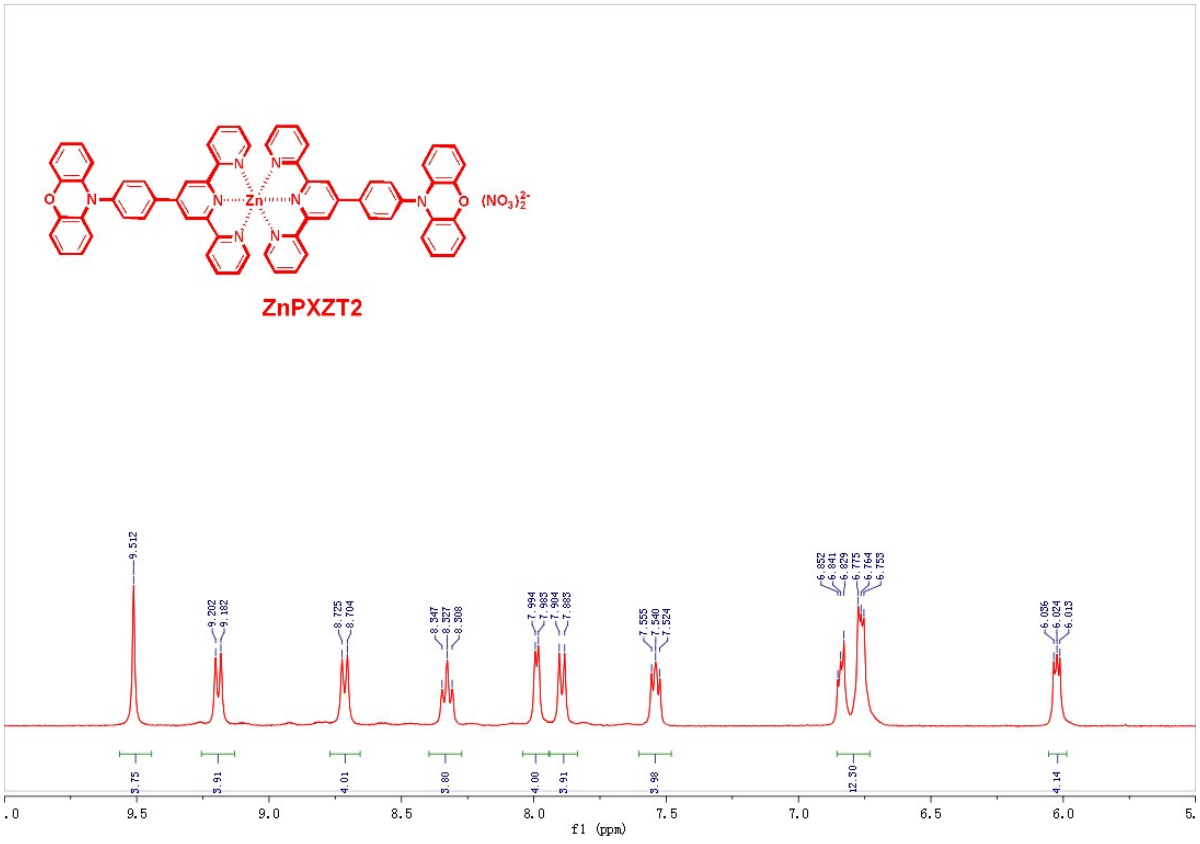
ZnPXZT2
(NO3)2
9.512
9.202
9.182
8.725
8.704
8.347
8.327
8.308
7.994
7.983
7.904
7.883
7.555
7.540
7.524
6.852
6.841
6.829
6.775
6.764
6.753
6.036
6.024
6.013
3.75
3.91
4.01
3.80
4.00
3.91
3.98
12.30
4.14
f1 (ppm)

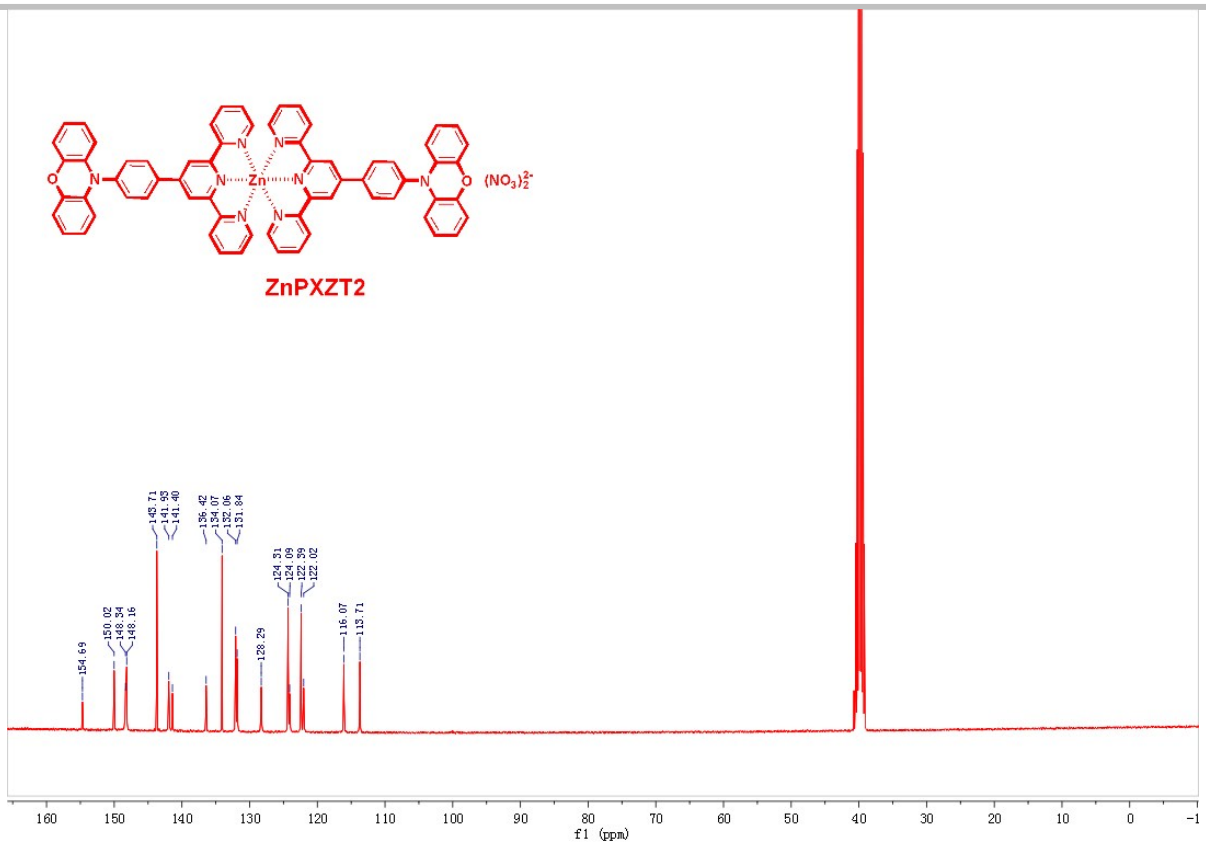
ZnPXZT2
154.69
150.02
148.34
148.16
143.71
141.93
141.40
136.42
134.07
132.06
131.84
128.29
124.31
124.09
122.39
122.02
116.07
113.71
f1 (ppm)

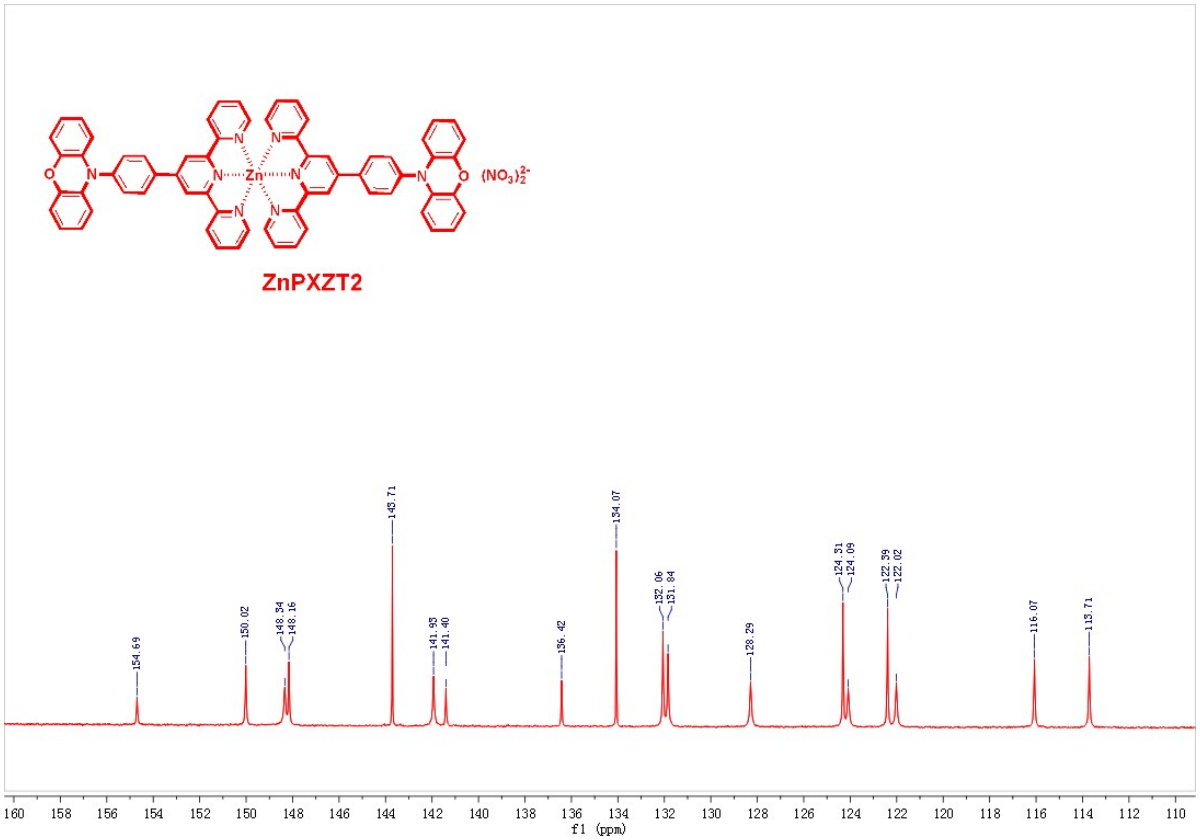
ZnPXZT2
154.69
150.02
148.34
148.16
143.71
141.93
141.40
136.42
134.07
132.06
131.84
128.29
124.31
124.09
122.39
122.02
116.07
113.71
f1 (ppm)

High resolution mass spectrometry of PXZT, ZnPXZT1 and ZnPXZT2

PXZT: HRMS (ESI) m/z calcd for $C_{33}H_{23}N_4O^+$ $(M+H)^+$ 491.18664, found 491.18640.

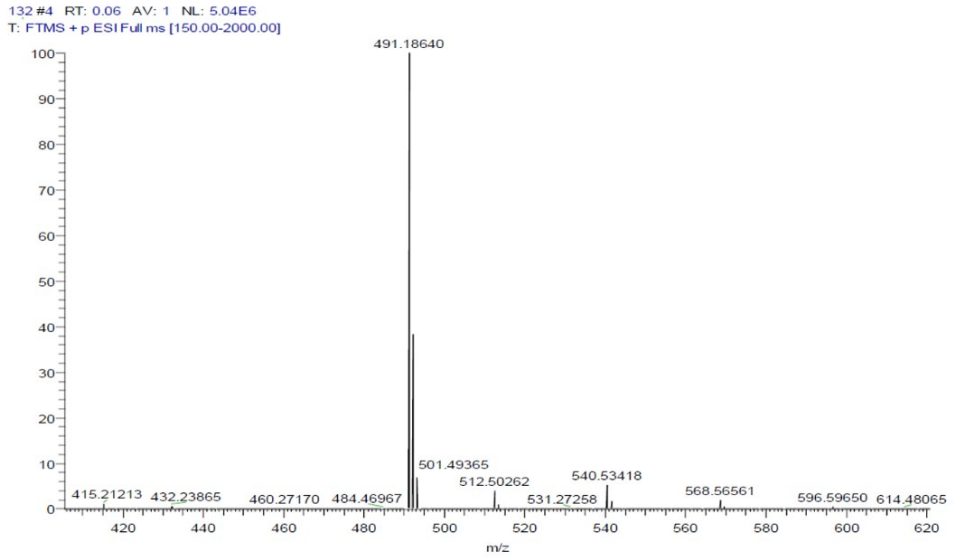

ZnPXZT1: HRMS (ESI) m/z calcd for $C_{33}H_{23}N_4OZn^{2+}$ $(M+H)^+$ 277.05371, found 277.05316.

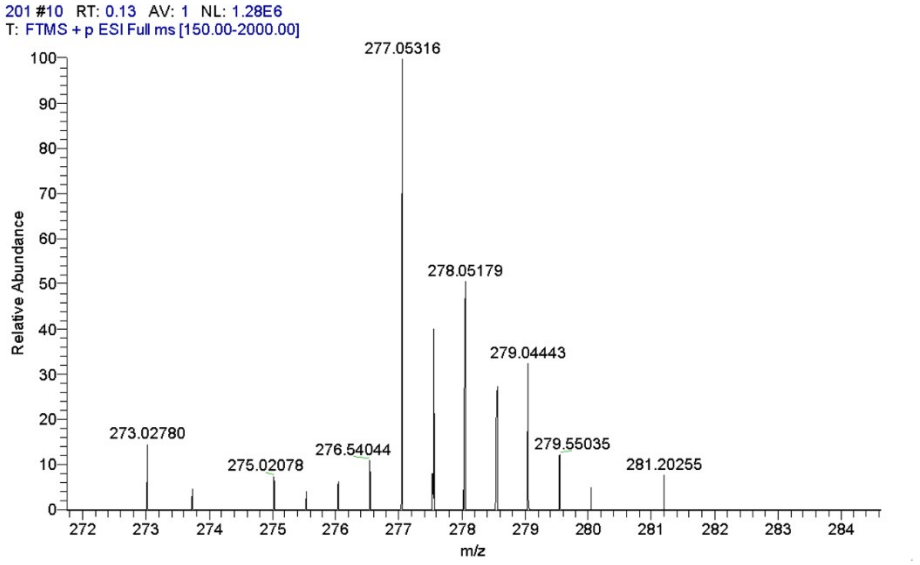

ZnPXZT2: HRMS (ESI) m/z calcd for calcd for $C_{66}H_{44}N_8O_2Zn^{2+}$ $(M)^{2+}$ 522.14339, found 522.14374.

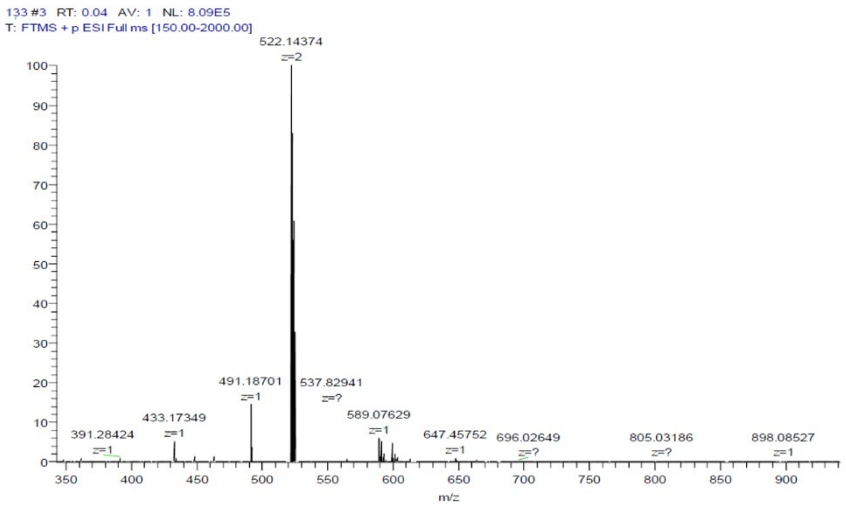

The crystal data of PXZT, ZnPXZT1 and ZnPXZT2

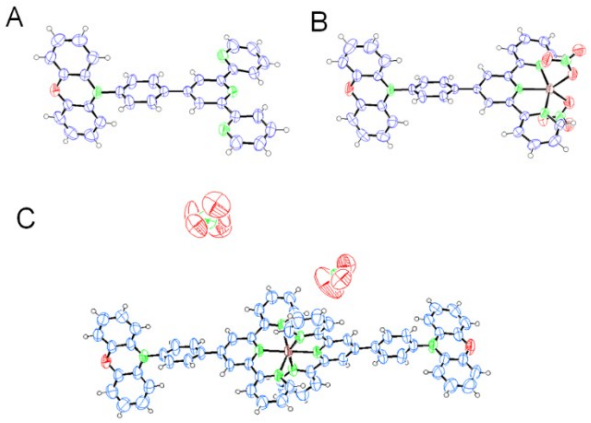

(a)-(c) The ORTEP drawing of single crystal structure of PXZT, ZnPXZT1 and ZnPXZT2 (CCDC number: 1497984, 1497985, 1497986). Colour code: carbon = blue, hydrogen = white, nitrogen = green, oxygen = red, zinc = purple.

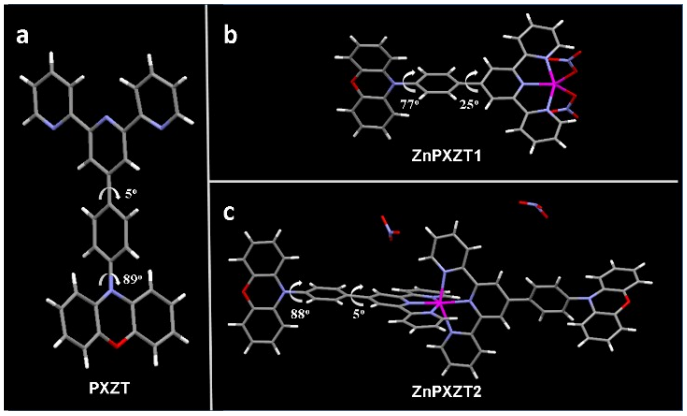

(a)-(c) Molecular structures of PXZT, ZnPXZT1 and ZnPXZT2. Colour code: carbon = grey, hydrogen = white, nitrogen = blue, oxygen = red, zinc = pink.

Crystal data	PXZT	ZnPXZT1	ZnPXZT2
Cell parameters			
Formula	$C_{33}H_{22}N_4O$	$C_{33}H_{22}N_6O_7Zn$	$C_{66}H_{44}N_8O_2Zn,2(NO_3)$
Formula Weight	490.55	679.96	1170.50
a (Å)	9.3334(15)	10.4399(14)	13.3069(5)
b (Å)	19.560(3)	11.3331(15)	18.6034(9)
c (Å)	13.636(2)	13.2139(18)	27.4104(12)
α (◦)	90	100.001(2)	90
β (◦)	94.259(5)	99.774(2)	102.321(2)
γ (◦)	90	99.056(2)	90
V (Å^3)	2482.7(7)	1488.9(3)	6629.3(5)
Space Group	P 21/c	P -1	P 21/c
Hall Group	-P 2ybc	-P 1	-P 2ybc

Crystal System	monoclinic	triclinic	monoclinic
F000	1024.0	696.0	2416.0
Data Collection			
Temperature	296K	293K	293K
Radiation	MoKα 0.71073	MoKα 0.71073	CuKα 1.54178
θmin/θmax (°)	1.8/28.7	1.6/26.3	2.9/65.8
h/k/lmax	12/26/18	12/14/16	15/21/32
Total Data	44104	11605	51290
Unique Data	6395	5915	11216
R(int)	0.026	0.041	0.068
Observed Data [I > 2.0 θ(I)]	4091	3955	8292
Refinement			
No. of Reflections	6395	5908	11216
No. of Refined Par.	343	424	794
R	0.0465	0.0506	0.0625
wR2	0.1448	0.1717	0.2004
S	1.04	1.00	1.10
Max. and Av. Shift/Error	0.00, 0.00	0.00, 0.00	0.01, 0.00
Min. and Max. Resd. Dens.	-0.18, 0.15	-0.35, 0.45	-0.45, 0.65